VIP Concave Nanocrystals Very Important Paper

DOI: 10.1002/anie.201307518

Highly Concave Platinum Nanoframes with High-Index Facets and Enhanced Electrocatalytic Properties**

Bao Yu Xia, Hao Bin Wu, Xin Wang, and Xiong Wen (David) Lou**

Platinum is the major component of many industrially important catalysts in environmental and energy applications.[1] For example, it is the active component of the catalysts in catalytic converters of automobiles and low-temperature fuel cells. The catalytic performance depends highly on the surface properties of synthesized Pt nanocrystals.[2] Therefore, enormous amount of effort has been devoted to synthesize unconventionally shaped Pt nanocrystals,[3] especially those bounded with well-defined and high-index facets.[4] These high-index facets possess a high density of lowly coordinated atoms which usually serve as more-active catalytic sites, thus resulting in enhanced catalytic performance in comparison with their low-index counterparts.[5] Although there have been many successes in preparing such nanocrystals with high-index facets, most of them are polyhedrons with convex surfaces.[6] On the other hand, concave nanocrystals, having open negative curvature and high-index facets, are expected to show substantially enhanced properties relative to their convex counterparts.[7] However, formation of concave surfaces with negative curvature is not favored by thermodynamics owing to the higher surface energy and inner strain.[8] Compared to the site-specific dissolution strategy,[9] directionally controlled overgrowth assisted by capping agents provides an easier way to generate nanocrystals with concave surfaces.[10] The capping agents can selectively bind to some specific facets and alter the relative growth rates, hence make the formation of concave nanocrystals with negative curvature thermodynamically favorable.[11] In spite of several reports claiming successful preparation of concave Pt nanocrystals,[11c,12] the real surface structures are not very clear yet, and the adsorption/desorption of hydrogen and oxygen on the Pt concave nanostructures does not show well-defined voltammetric features.[5b,c] Therefore, it remains challenging to synthesize Pt nanocrystals with high-index facets and open concave surfaces to maximize the amount of active surface sites while decreasing the usage of noble metals in catalysts.[13]

Herein, we report the synthesis, characterization, and electrochemical measurement of highly concave Pt nanoframes prepared by a simple solution method (see Supporting Information). Compared with previously reported concave Pt nanocrystals, the as-prepared Pt nanoframes have a much deeper concavity and are enclosed by high-index {740} facets. Such highly concave structures provide more-active surface structures such as atomic steps, kinks, corners, and edges, and at the same time maximize the surface area to volume ratio. This situation will reduce the catalyst loading and simultaneously enhance the catalytic performance. Furthermore, the negative and open surface structure can facilitate the mass exchange and chemical reactions. Because of their many advantages, such highly concave Pt nanoframes exhibit excellent activity and remarkable stability relative to Pt nanocubes enclosed by (100) facets and commercial Pt/C electrocatalysts.

Figure 1 a shows a representative field-emission scanning electron microscopy (FESEM) image of Pt nanoframes. The as-prepared Pt nanoframes are highly uniform with an average size of about 60 nm. The higher magnification FESEM image (Inset of Figure 1 a) clearly shows that the Pt nanoframes with a cubic shape have a highly concave structure. Energy-dispersive X-ray (EDX) and X-ray diffraction (XRD) analyses confirm that the as-prepared samples consist exclusively of Pt (see Supporting Information, Figure S1 and S2) with a face centered cubic (*fcc*) structure. The morphology and structure of the concave nanoframes are further characterized by transmission electron microscopy (TEM). TEM images (Figure 1 b) show that each nanoframe exhibits a dark star contrast in the diagonal section as compared to the edges and center regions. This indicates the clear features of curving in or hollowing of the surface. By measuring the angles of several highly concave Pt nanoframes, the concavity of the Pt nanoframes is around 30° from the sides of nanoframes (Figure 1 c1). On the basis of the geometric shape of nanoframes, it might be deduced that the surface of a concave Pt nanoframe is nominally enclosed by {740} facets. The proposed highly concave and three-dimensional (3D) structure is confirmed by high-resolution (HR) TEM. Figure 1 c1 and inset, show an individual Pt nanoframe with starlike core projected from the [001] direction and its corresponding geometrical model viewed from the top, respectively. The depression of the nanoframes is also measured as 30° viewed along [001] zone axis. Both HRTEM and selected-area electron diffraction (SAED; Figure 1 c2) measurements on the individual Pt nanoframe clearly reveal the single-crystalline structure. As confirmed by

[*] Dr. B. Y. Xia, H. B. Wu, Prof. X. Wang, Prof. X. W. Lou
School of Chemical and Biomedical Engineering
Nanyang Technological University
62 Nanyang Drive, Singapore 637459 (Singapore)
E-mail: wangxin@ntu.edu.sg
xwlou@ntu.edu.sg
Homepage: http://www.ntu.edu.sg/home/xwlou/

[**] We acknowledge financial support from the Ministry of Education, Singapore through the academic research fund AcRF tier 2 (MOE2009-T2-2-024) and AcRF tier 1 (M4011020 RG8/12) and from the National Research Foundation, Singapore through the competitive research program (2009 NRF-CRP 001-032).

Supporting information for this article (detailed experimental procedure, FESEM and TEM images, XRD patterns and EDX results, electrochemical measurements) is available on the WWW under http://dx.doi.org/10.1002/anie.201307518.

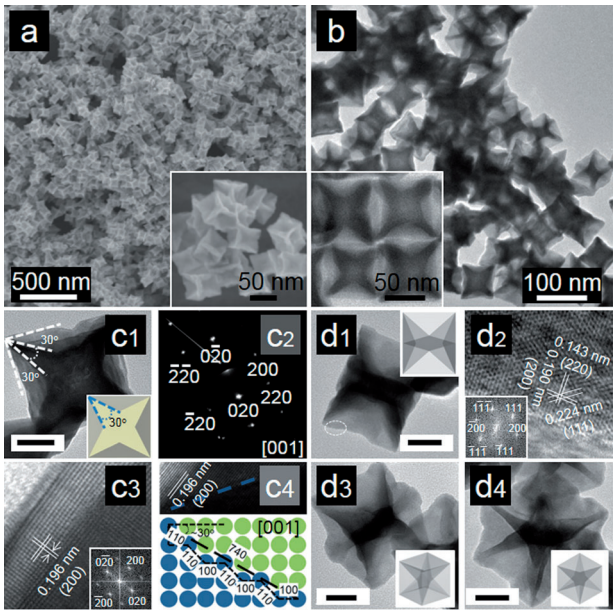

Figure 1. FESEM (a) and TEM (b) images of the highly concave Pt nanoframes. Insets: enlarged images. HRTEM image (c1) of an individual highly concave Pt nanoframe projected from the [100] direction. SAED pattern (c2). Enlarged HRTEM image (c3), Inset: corresponding fast Fourier transform (FFT) pattern. Enlarged HRTEM image (c4, top) taken from the corner of a concave frame, and illustration (c4, bottom) of the atomic arrangement on the {740} surface. Side view (d1) and corner view (d3 and d4) of a Pt nanoframe. Insets (c1, d1, d3, and d4) correspond to geometric models viewed from different directions of the concave Pt nanoframes. HRTEM image (d2) taken from the area in (d1) marked by the circle. Inset (d2) the FFT pattern. The scale bars in c1, d1, d3, and d4 are 20 nm.

the HRTEM image and corresponding fast Fourier transform (FFT) pattern in Figure 1 c3, the clear crystal lattice demonstrates the good crystallinity. Although it is still a challenge to provide the evidence of the surface atomic arrangement by HRTEM examination owing to the concave shape and the covered edges of Pt nanoframes, a direct identification of the negative curvature on one corner is given in Figure 1 c4 (top). Figure 1 c4 (bottom) shows the two-dimensional (2D) atomic model, demonstrating the {740} terrace step structures consisting of (100) and (110) terraces and steps. Compared with previously reported concave Pt and Au nanocubes that are enclosed mostly by {720} planes,[7b,11b,c,12] the present Pt nanoframes exhibit much deeper depression and more highly concave structure. As the concavity becomes larger, the density of the steps on the open structure increases, and more corners, edges, kinks are formed simultaneously. Figure 1 d presents nanoframes and the corresponding geometric models viewed from different directions. The stereoscopic models can directly show the structure of nanoframes with negative depression on six surfaces. Each facet of a convex nanocrystal can be intuitively described as a pyramid, which is pulling out from the center.[5d] In contrast, the present Pt nanoframes are formed by excavating out a square pyramid from each (100) surface of a cube (Figure 1 d). It should be pointed out that all the surfaces of these concave nanoframes are composed of similar high-index facets (Figure 1). A simple geometrical analysis suggests that the surface area of the present nanoframes increases 2.3 times and the volume decreases to 57% compared to that of nanocubes with the same size, which leads to the increase of the surface area to volume ratio by about 4 times. The concave nanoframes form a more open negative curvature surface. This structure would be helpful for the enhanced interaction between the reactant and catalyst surface, thus resulting in higher electrocatalytic activity.[14]

The use of oleylamine (OAm) is critical to control the shape and exposed surface in the synthesis process. In the absence of OAm, only irregular spherical Pt nanoparticles are obtained (Supporting information, Figure S3a). With the addition of small amount of OAm (10%), cubic Pt nanocrystals are obtained with the size increased to about 20 nm (Figure 2 a and Supporting Information, Figure S3b). This

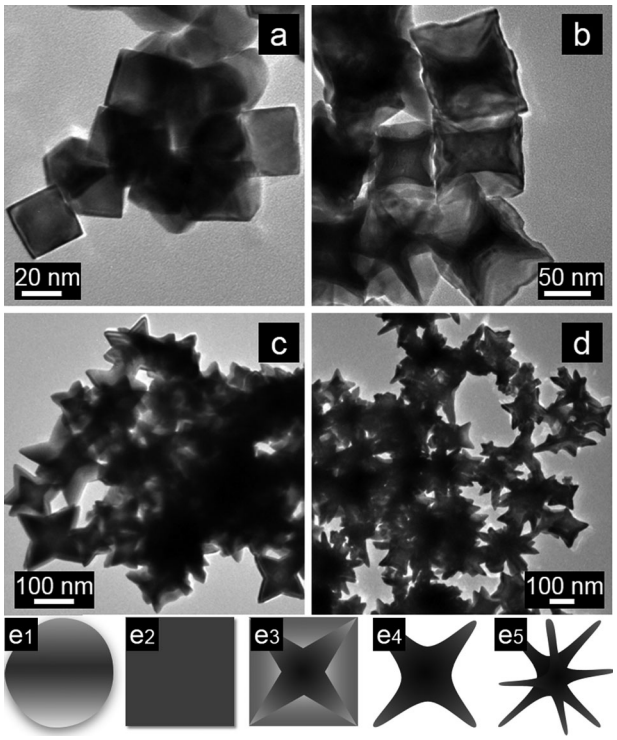

Figure 2. TEM images of Pt nanocrystals obtained with different volume fractions of OAm. a) 10%; b) 20%; c) 40%; d) 60%. e1–e5) show the illustration of shape evolution with the increase of OAm.

observation of shape evolution is similar to the synthesis of Pt nanocubes with the assistance of polyvinylpyrrolidone (PVP) or other organic species.[11a,e,15] With the increase of OAm (20%), well-developed concave Pt nanoframes can be obtained (Figure 2 b). However, Pt octapod nanocrystals are formed when the OAm amount is further increased to 40% (Figure 2 c and Supporting Information, Figure S3c). With the further increase of OAm (60%), more Pt octapod nanocrystals along with some multibranched Pt nanocrystals can be observed in the product (Figure 2 d and Supporting Information, Figure S3d). OAm is often used in the preparation of Au nanowires and multibranched Pt nanocrystals.[16] It

is proposed that the selective chemisorption of long-chain OAm molecules on the (100) surface of the initially formed Pt nanoparticles would induce the preferential overgrowth along ⟨110⟩ and ⟨111⟩ directions, thus facilitating the formation of concave nanostructures. With the addition of more OAm, pod or wire shaped products would form more favorably. Therefore, the selective binding on the specific facets would affect the relative overgrowth rate along different directions and thus result in the morphology evolution from particles to cubes, concave frames, octapods, and even multibranched nanocrystals along with the increase of OAm (Figure 2e).

The morphological evolution of Pt nanoframes during the solvothermal reaction is also examined by FESEM and TEM techniques (Supporting Information, Figure S4). The results indicate that the overgrowth occurs very fast on the initially formed Pt seeds along their corners and edges, namely ⟨111⟩ and ⟨110⟩ directions, respectively, thus leading to the formation of a highly concave structure. The observation of small multipod and trigonal Pt nanocrystals also suggests that the possibility of homogeneous nucleation and preferential growth along the Pt ⟨111⟩ direction. This confirms the formation mechanism that mainly involves the difference in the growth rate on {111} and {100} facets through the selective bindings of OAm on Pt nanocrystals.[11a,e,16d]

Highly concave Pt nanoframes with high-index facets can also be characterized by surface-sensitive electrochemical measurements.[17] Figure 3a shows the cyclic voltammetry (CV) profiles of the as-prepared Pt nanocubes and nanoframes, and commercial Pt/C (Johnson Matthey, JM 20 wt%) catalysts, in H_2SO_4 solution. The commercial Pt/C catalyst only exhibits a hydrogen desorption peak at about −0.13 V because of the lack of long-range order which is a result of the small Pt particle size. There is a clear desorption peak for Pt nanocubes at about −0.05 V which corresponds to Pt(100) terrace surface with long-range order.[17b,18] However, the same peak for Pt nanoframes only appears as a weak shoulder peak, indicating the existence of only small amount of long-range ordered Pt(100) terraces. Instead, two prominent peaks at approximately 0.01 V and about −0.13 V are observed for the Pt nanoframes. The enhanced peak at 0.01 V reveals that Pt nanoframes are rich in Pt(100) with short-range order in the forms of corners and edges, which is consistent with the presence of {740} facets. Note that the peak at about −0.13 V is mainly caused by the step structure of (110) facets on the high-index surface.[18] Therefore, the intense peak at about −0.13 V for Pt nanoframes also indicates the presence of many steps and terraces with short-range order on the surface, in good agreement with the atomic structure of Pt nanoframes with exposed {740} surface. Moreover, a larger current associated with the adsorption/desorption of oxygen containing species can be observed on Pt nanoframes in the potential range of 0.4–0.75 V, which reveals a higher density of Pt atomic steps on the surface of Pt nanoframes over Pt nanocubes and commercial Pt/C catalysts.[19] The calculated specific electrochemical surface area (ECSA) of Pt nanoframes is 42.1 $m^2 g^{-1}$, which is about 65% and 76% of that of the commercial Pt/C catalyst (64.8 $m^2 g^{-1}$) and Pt nanocubes (55.7 $m^2 g^{-1}$), respectively. The lower ECSA of Pt nanoframes is most likely due to the presence of residual impurities adsorbed on the surface and the larger size (ca. 60 nm) compared with Pt nanoparticles (ca. 3 nm) in commercial catalysts and Pt nanocubes (ca. 20 nm). Next, the electrocatalytic activity for the oxygen reduction reaction (ORR) is evaluated, as shown in Figure 3b. The half-wave potentials of Pt nanoframes, Pt nanocubes, and commercial Pt/C catalysts are 0.834, 0.816, and 0.80 V (vs. a reversible hydrogen electrode (RHE)), respectively. This shows that the activity of the Pt nanoframes is higher than that of Pt nanocubes and commercial Pt/C catalysts. Mass and specific activities are important parameters of electrocatalysts. Pt nanoframes exhibit a mass activity of 13.1 $A g^{-1}$ Pt at 0.80 V, which is about 1.22 and 1.68 times of that of Pt nanocubes and commercial Pt/C catalysts, respectively. Despite having a lower ECSA, the specific ORR activity of Pt nanoframes is 1.60 and 2.62 times of that of Pt nanocubes and commercial Pt/C catalysts, respectively (Figure 3c). Furthermore, the accelerated CV measurement is carried out to evaluate the catalytic stability. After 5000 cycles, the CV profile still remains largely unchanged for concave Pt nanoframes (Figure 3d). TEM characterization also shows that Pt nanoframes retain the well-defined concave morphology after the long-term durability test (Supporting Information, Figure S5). Despite the possible surface atomic rearrangement, the retained concave surface and higher electrochemical stability could be attributed to the good crystallinity of Pt nanoframes with large size. On the contrary, the commercial Pt/C electrocatalyst shows a remarkable current density loss over 3000 cycles (Supporting Information, Figure S6), which is in part ascribed to the dissolution/aggregation of Pt and corrosion of

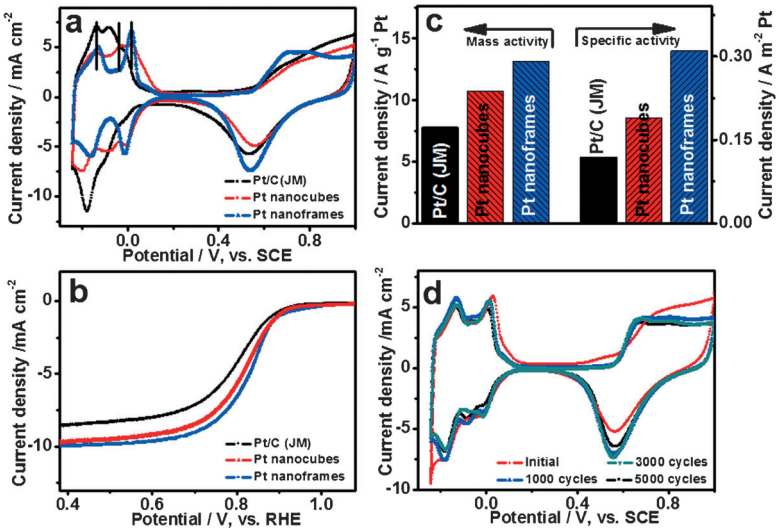

Figure 3. a) Cyclic voltammetric curves of different Pt catalysts recorded in 0.5 M H_2SO_4 solution with the scan rate of 20 $mV s^{-1}$. b) Polarization curves for ORR in an O_2 saturated 0.5 M H_2SO_4 solution (1600 rpm; sweep rate: 10 $mV s^{-1}$). c) The mass and specific activities (at 0.8 V vs. RHE). d) Electrochemical durability test of concave Pt nanoframes in 0.5 M H_2SO_4 solution with a sweep rate of 20 $mV s^{-1}$.

carbon supports.[20] Pt nanoframes and commercial Pt/C catalysts are also evaluated as electrocatalysts to oxidize organic fuels, such as methanol and formic acid (Supporting Information, Figure S7). It is apparent that Pt nanoframes have a superior catalytic activity and stability than the commercial Pt/C catalyst.

In summary, highly concave Pt nanoframes enclosed by {740} facets have been prepared by a one-pot solvothermal method. An appropriate amount of OAm in the reaction solution is crucial for the formation of highly concave Pt nanostructures. The Pt nanoframes with highly negative curvature surface have a higher percentage of step, corner, and edge sites. When evaluated as the electrocatalysts for the oxygen reduction reaction and oxidation of small fuel molecules, the Pt nanoframes have a higher electrochemical activity and significantly improved long-term stability compared to the commercial Pt/C catalyst. The excellent electrocatalytic performance would be ascribed to the unique nanostructure which contains high-index facets and an open negative surface.

Received: August 27, 2013
Published online: September 25, 2013

Keywords: concave surface · electrocatalysis · high-index facets · nanocrystals · platinum

[1] a) V. R. Stamenkovic, B. S. Mun, M. Arenz, K. J. J. Mayrhofer, C. A. Lucas, G. F. Wang, P. N. Ross, N. M. Markovic, *Nat. Mater.* **2007**, *6*, 241; b) S. Polarz, *Adv. Funct. Mater.* **2011**, *21*, 3214.

[2] a) T. S. Ahmadi, Z. L. Wang, T. C. Green, A. Henglein, M. A. El-Sayed, *Science* **1996**, *272*, 1924; b) K. Zhou, Y. Li, *Angew. Chem.* **2012**, *124*, 622; *Angew. Chem. Int. Ed.* **2012**, *51*, 602; c) K. An, G. A. Somorjai, *ChemCatChem* **2012**, *4*, 1512; d) B. Y. Xia, H. B. Wu, Y. Yan, X. W. Lou, X. Wang, *J. Am. Chem. Soc.* **2013**, *135*, 9480.

[3] Y. Xia, Y. Xiong, B. Lim, S. E. Skrabalak, *Angew. Chem.* **2009**, *121*, 62; *Angew. Chem. Int. Ed.* **2009**, *48*, 60.

[4] a) N. Tian, Z.-Y. Zhou, S.-G. Sun, Y. Ding, Z. L. Wang, *Science* **2007**, *316*, 732; b) Y. Xiong, B. Wiley, Y. Xia, *Angew. Chem.* **2007**, *119*, 7291; *Angew. Chem. Int. Ed.* **2007**, *46*, 7157; c) W. Niu, G. Xu, *Nano Today* **2011**, *6*, 265; d) J. Wu, L. Qi, H. You, A. Gross, J. Li, H. Yang, *J. Am. Chem. Soc.* **2012**, *134*, 11880; e) H. Zhang, M. Jin, Y. Xiong, B. Lim, Y. Xia, *Acc. Chem. Res.* **2013**, *46*, 1783.

[5] a) Y. Y. Ma, Q. Kuang, Z. Y. Jiang, Z. X. Xie, R. B. Huang, L. S. Zheng, *Angew. Chem.* **2008**, *120*, 9033; *Angew. Chem. Int. Ed.* **2008**, *47*, 8901; b) Z. Y. Zhou, N. Tian, J. T. Li, I. Broadwell, S. G. Sun, *Chem. Soc. Rev.* **2011**, *40*, 4167; c) H. You, S. Yang, B. Ding, H. Yang, *Chem. Soc. Rev.* **2013**, *42*, 2880; d) Z. Quan, Y. Wang, J. Fang, *Acc. Chem. Res.* **2013**, *46*, 191.

[6] a) T. Ming, W. Feng, Q. Tang, F. Wang, L. D. Sun, J. F. Wang, C. H. Yan, *J. Am. Chem. Soc.* **2009**, *131*, 16350; b) Y. Yu, Q. B. Zhang, B. Liu, J. Y. Lee, *J. Am. Chem. Soc.* **2010**, *132*, 18258; c) L. Zhang, J. W. Zhang, Q. Kuang, S. F. Xie, Z. Y. Jiang, Z. X. Xie, L. S. Zheng, *J. Am. Chem. Soc.* **2011**, *133*, 17114; d) Y. Yamada, C. K. Tsung, W. Huang, Z. Huo, S. E. Habas, T. Soejima, C. E. Aliaga, G. A. Somorjai, P. Yang, *Nat. Chem.* **2011**, *3*, 372; e) D. Kim, Y. W. Lee, S. B. Lee, S. W. Han, *Angew. Chem.* **2012**, *124*, 163; *Angew. Chem. Int. Ed.* **2012**, *51*, 159.

[7] a) X. Q. Huang, S. H. Tang, H. H. Zhang, Z. Y. Zhou, N. F. Zheng, *J. Am. Chem. Soc.* **2009**, *131*, 13916; b) J. A. Zhang, M. R. Langille, M. L. Personick, K. Zhang, S. Y. Li, C. A. Mirkin, *J. Am. Chem. Soc.* **2010**, *132*, 14012; c) X. H. Xia, J. Zeng, B. McDearmon, Y. Q. Zheng, Q. G. Li, Y. N. Xia, *Angew. Chem.* **2011**, *123*, 12750; *Angew. Chem. Int. Ed.* **2011**, *50*, 12542; d) C. J. DeSantis, A. A. Peverly, D. G. Peters, S. E. Skrabalak, *Nano Lett.* **2011**, *11*, 2164; e) M. R. Langille, M. L. Personick, J. Zhang, C. A. Mirkin, *J. Am. Chem. Soc.* **2011**, *133*, 10414; f) F. Wang, C. H. Li, L. D. Sun, H. S. Wu, T. A. Ming, J. F. Wang, J. C. Yu, C. H. Yan, *J. Am. Chem. Soc.* **2011**, *133*, 1106; g) L. F. Zhang, S. L. Zhong, A. W. Xu, *Angew. Chem.* **2013**, *125*, 673; *Angew. Chem. Int. Ed.* **2013**, *52*, 645.

[8] H. Zhang, M. S. Jin, Y. N. Xia, *Angew. Chem.* **2012**, *124*, 7774; *Angew. Chem. Int. Ed.* **2012**, *51*, 7656.

[9] a) S. Cheong, J. Watt, B. Ingham, M. F. Toney, R. D. Tilley, *J. Am. Chem. Soc.* **2009**, *131*, 14590; b) S. F. Xie, N. Lu, Z. X. Xie, J. G. Wang, M. J. Kim, Y. N. Xia, *Angew. Chem.* **2012**, *124*, 10412; *Angew. Chem. Int. Ed.* **2012**, *51*, 10266; c) G. Chen, Y. Tan, B. Wu, G. Fu, N. Zheng, *Chem. Commun.* **2012**, *48*, 2758.

[10] M. Chen, B. H. Wu, J. Yang, N. F. Zheng, *Adv. Mater.* **2012**, *24*, 862.

[11] a) Y. J. Li, Y. Huang, *Adv. Mater.* **2010**, *22*, 1921; b) M. S. Jin, H. Zhang, Z. X. Xie, Y. N. Xia, *Angew. Chem.* **2011**, *123*, 7996; *Angew. Chem. Int. Ed.* **2011**, *50*, 7850; c) T. Yu, D. Y. Kim, H. Zhang, Y. N. Xia, *Angew. Chem.* **2011**, *123*, 2825; *Angew. Chem. Int. Ed.* **2011**, *50*, 2773; d) X. Huang, Z. Zhao, J. Fan, Y. Tan, N. Zheng, *J. Am. Chem. Soc.* **2011**, *133*, 4718; e) C. Y. Chiu, Y. J. Li, L. Y. Ruan, X. C. Ye, C. B. Murray, Y. Huang, *Nat. Chem.* **2011**, *3*, 393; f) J. W. Zhang, L. Zhang, S. F. Xie, Q. Kuang, X. G. Han, Z. X. Xie, L. S. Zheng, *Chem. Eur. J.* **2011**, *17*, 9915.

[12] Z. C. Zhang, J. F. Hui, Z. C. Liu, X. Zhang, J. Zhuang, X. Wang, *Langmuir* **2012**, *28*, 14845.

[13] D. L. Feldheim, *Science* **2007**, *316*, 699.

[14] Z. L. Wang, T. S. Ahmad, M. A. El-Sayed, *Surf. Sci.* **1997**, *380*, 302.

[15] H. Lee, S. E. Habas, S. Kweskin, D. Butcher, G. a. Somorjai, P. Yang, *Angew. Chem.* **2006**, *118*, 7988; *Angew. Chem. Int. Ed.* **2006**, *45*, 7824.

[16] a) Z. Huo, C.-k. Tsung, W. Huang, X. Zhang, P. Yang, *Nano Lett.* **2008**, *8*, 2041; b) B. Lim, Y. Xia, *Angew. Chem.* **2011**, *123*, 78; *Angew. Chem. Int. Ed.* **2011**, *50*, 76; c) L. Zhang, D. Q. Chen, Z. Y. Jiang, J. W. Zhang, S. F. Xie, Q. Kuang, Z. X. Xie, L. S. Zheng, *Nano Res.* **2012**, *5*, 181; d) B. Y. Xia, W. T. Ng, H. B. Wu, X. Wang, X. W. Lou, *Angew. Chem.* **2012**, *124*, 7325; *Angew. Chem. Int. Ed.* **2012**, *51*, 7213; e) L.-M. Lacroix, C. Gatel, R. Arenal, C. Garcia, S. Lachaize, T. Blon, B. Warot-Fonrose, E. Snoeck, B. Chaudret, G. Viau, *Angew. Chem.* **2012**, *124*, 4768; *Angew. Chem. Int. Ed.* **2012**, *51*, 4690; f) S. Mourdikoudis, L. M. Liz-Marzán, *Chem. Mater.* **2013**, *25*, 1465.

[17] a) V. R. Stamenkovic, B. Fowler, B. S. Mun, G. Wang, P. N. Ross, C. A. Lucas, N. M. Marković, *Science* **2007**, *315*, 493; b) C. Wang, H. Daimon, T. Onodera, T. Koda, S. Sun, *Angew. Chem.* **2008**, *120*, 3644; *Angew. Chem. Int. Ed.* **2008**, *47*, 3588; c) F. J. Vidal-Iglesias, R. M. Aran-Ais, J. Solla-Gullon, E. Herrero, J. M. Feliu, *ACS Catal.* **2012**, *2*, 901.

[18] J. Solla-Gullón, P. Rodríguez, E. Herrero, A. Aldaz, J. M. Feliu, *Phys. Chem. Chem. Phys.* **2008**, *10*, 1359.

[19] Z. Y. Zhou, Z. Z. Huang, D. J. Chen, Q. Wang, N. Tian, S. G. Sun, *Angew. Chem.* **2010**, *122*, 421; *Angew. Chem. Int. Ed.* **2010**, *49*, 411.

[20] X. Wang, W. Li, Z. Chen, M. Waje, Y. Yan, *J. Power Sources* **2006**, *158*, 154.

